MOLECULAR IMAGING AND BIOLOGY

Mol Imaging Biol (2016) 18:807–819
DOI: 10.1007/s11307-016-0959-4

Published Online: 29 April 2016

RESEARCH ARTICLE

Selecting Tumor-Specific Molecular Targets in Pancreatic Adenocarcinoma: Paving the Way for Image-Guided Pancreatic Surgery

Susanna W. L. de Geus,[1] Leonora S. F. Boogerd,[1] Rutger-Jan Swijnenburg,[1] J. Sven D. Mieog,[1] Willemieke S. F. J. Tummers,[1] Hendrica A. J. M. Prevoo,[1] Cornelis F. M. Sier,[1] Hans Morreau,[2] Bert A. Bonsing,[1] Cornelis J. H. van de Velde,[1] Alexander L. Vahrmeijer,[1] Peter J. K. Kuppen[1]

[1]*Department of Surgery, Leiden University Medical Center, Albinusdreef 2, 2300 RC, Leiden, The Netherlands*
[2]*Department of Pathology, Leiden University Medical Center, Leiden, The Netherlands*

Abstract

Purpose: The purpose of this study was to identify suitable molecular targets for tumor-specific imaging of pancreatic adenocarcinoma.

Procedures: The expression of eight potential imaging targets was assessed by the target selection criteria (TASC)—score and immunohistochemical analysis in normal pancreatic tissue ($n=9$), pancreatic ($n=137$), and periampullary ($n=28$) adenocarcinoma.

Results: Integrin $\alpha_v\beta_6$, carcinoembryonic antigen (CEA), epithelial growth factor receptor (EGFR), and urokinase plasminogen activator receptor (uPAR) showed a significantly higher (all $p<0.001$) expression in pancreatic adenocarcinoma compared to normal pancreatic tissue and were confirmed by the TASC score as promising imaging targets. Furthermore, these biomarkers were expressed in respectively 88 %, 71 %, 69 %, and 67 % of the pancreatic adenocarcinoma patients.

Conclusions: The results of this study show that integrin $\alpha_v\beta_6$, CEA, EGFR, and uPAR are suitable targets for tumor-specific imaging of pancreatic adenocarcinoma.

Key words: Pancreatic adenocarcinoma, Periampullary adenocarcinoma, Molecular imaging, Image-guided surgery, Immunohistochemistry, Integrin $\alpha_v\beta_6$, Carcinoembryonic antigen (CEA), Epithelial growth factor receptor (EGFR), Urokinase plasminogen activator receptor (uPAR)

Introduction

Pancreatic adenocarcinoma currently ranks the fourth leading cause of cancer-related death in the Western world, with a 5-year survival rate of less than 5 % [1]. Radical surgical tumor resection is imperative to curative treatment of these patients as positive resection margins (defined as tumor cells present at the surface of the resection margins of the surgical specimen) are associated with a dramatic decrease in median overall survival [1–4]. Unfortunately, positive resection margins are common after pancreatic surgery and reported rates vary between 24 % and 76 % [5–7]. Adjuvant therapy cannot retaliate the poor survival outcome associated with residual disease [8]. The disappointing irradical resection rates after pancreatic surgery are due to our current inability to detect the true delineation of the tumor extent during surgery, which is further complicated by the intricate anatomy of the pancreas and the commonly

Correspondence to: Peter Kuppen; *e-mail:* p.j.k.kuppen@lumc.nl

present peritumoral inflammatory zone in pancreatic cancer. Conventional anatomic imaging modalities used for preoperative diagnosis, staging, and surgical planning include multiphase intravenous contrast-directed thin slice computed tomography, magnetic resonance imaging, endoscopic ultrasonography, and endoscopic retrograde cholangiopancreatography [9, 10]. However, the translation of these preoperative imaging techniques to the surgical field remains challenging and in the theater, the surgical oncologist solely has to rely on vision and manual palpation to discriminate between malignant and healthy pancreatic tissue, assisted by ultrasonography and pathologic evaluation of frozen tissue sections [10].

Intraoperative tumor-specific imaging offers the opportunity to significantly improve current practice by increasing the capability to obtain negative resection margins and visualize residual disease during pancreatic surgery. This novel imaging approach uses labeled receptor ligands, nanoparticles, antibodies, or antibody fragments targeting cancer-specific antigens on the tumor surface detected by positron emission tomography, single-photon emission computed tomography, ultrasonography, magnetic resonance, and/or near-infrared fluorescence imaging modalities [11–13]. The feasibility of these imaging techniques has already successfully been proven in glioma and ovarian cancer surgery using respectively the fluorescent agents 5-aminolevulinic acid and folate conjugated to fluorescein isothiocyanate [11, 14]. Furthermore, the potential of image-guided surgery in pancreatic adenocarcinoma has been demonstrated by numerous preclinical studies using cancer-specific contrast agents targeting integrin $\alpha_v\beta_6$, carcinoembryonic antigen (CEA), epithelial growth factor receptor (EGFR), human epidermal growth factor receptor (HER2), urokinase plasminogen activator receptor (uPAR), or vascular endothelial growth factor receptor 2 (VEGFR2) among others (Table 1). Nevertheless, the orthotopic mouse models used in these studies are based on a small number of pancreatic adenocarcinoma cell lines originating from single patients and therefore less representative for the potential of these imaging probes in the overall population of pancreatic cancer patients. The translation from bench to bedside of this promising imaging strategy for pancreatic adenocarcinoma currently hinges on the lack of tumor-specific and thoroughly evaluated molecular targets expressed on the general population of pancreatic adenocarcinoma patients for the further development of tumor-targeting contrast agents [15, 16].

Therefore, the aim of this study was to explore the suitability of integrin $\alpha_v\beta_6$, CEA, hepatocyte growth factor receptor (cMET), EGFR, epithelial cell adhesion molecule (EpCAM), HER2, uPAR, and VEGFR2 as molecular targets for tumor-targeted imaging of pancreatic adenocarcinoma patients. The primary endpoint of this study was to evaluate the ability of these markers to distinguish between normal pancreatic tissue and pancreatic and periampullary adenocarcinoma by performing immunohistochemistry on surgical specimen of these malignancies and normal pancreatic tissue obtained adjacent to the tumor. In addition, these biomarkers were judged on the Target Selection Criteria (TASC) proposed by Van Oosten et al. [17].

Materials and Methods

Patient Selection

Medical records and pathology specimens of 137 patients with pancreatic ductal adenocarcinoma and 28 patients with periampullary adenocarcinoma who underwent pancreatic surgery at Leiden University Medical Center (LUMC) between June 2002 and July 2012 were retrospectively reviewed. Periampullary adenocarcinoma were included to assess the potential of tumor-specific imaging targets to visualize every pancreatic head mass, since preoperative differentiation between pancreatic, distal bile duct, ampullary, and duodenal adenocarcinoma can be challenging [18]. For the purpose of this study, periampullary adenocarcinoma was defined as adenocarcinoma that invades the pancreas arising from the ampulla of Vater, duodenum, or distal bile duct [19]. Patients who received any form of neoadjuvant chemotherapy and/or radiotherapy were excluded from this study, since this may influence the expression of molecular markers [20]. In addition, normal pancreatic tissue adjacent to the tumor was also obtained from nine patients to evaluate the tumor specificity of the biomarkers. Clinicopathological data from these patients were retrospectively collected from electronic hospital records. Tumor differentiation grade was determined according to the guideline of the World Health Organization, and the TNM stage was defined according to the American Joint Commission on Cancer criteria [21]. All samples were nonidentifiable and used in accordance with the ethical standards of the institutional research committee and with the 1964 Helsinki declaration and its later amendments.

Immunohistochemistry

Tissue microarrays (TMAs) of tumor and normal tissues were constructed to perform uniform and simultaneous immunohistochemical stainings to limit intra-assay variations. Formalin-fixed paraffin-embedded tissue blocks of the primary tumor were collected from the archives of the Pathology Department. A single representative block was selected for each patient based on hematoxylin-eosin-stained sections. From each donor block, triplicate 2.0-mm cores were punched from areas with clear histopathological tumor representation and transferred to a recipient TMA block using the TMA Master (3DHISTECH, Budapest, Hungary). From each completed TMA block and normal pancreatic tissue block,

Table 1. Overview of the characteristics and preclinical experience with tumor-specific imaging of integrin $\alpha_v\beta_6$, carcinoembryonic antigen (CEA), hepatocyte growth factor receptor (cMET), epithelial growth factor receptor (EGFR), epithelial cell adhesion molecule (EpCAM), human epidermal growth factor receptor (HER2), urokinase plasminogen activator receptor (uPAR), and vascular endothelial growth factor receptor 2 (VEGFR2) in pancreatic adenocarcinoma animal models

Target	Type of receptor (family)	Function	Tumor-specific probe		Imaging modality	Pancreatic cancer xenograft	Ref.
Integrin $\alpha_v\beta_6$	Transmembrane receptor (integrin family of cell adhesion receptors) [63]	Controls extracellular matrix remodeling and provides the traction necessary for cell motility. Tumor cell migration, invasion, and proliferation [63]	Peptide	^{18}F-fluorobenzoic acid	PET	BxPC-3	[64, 65]
			Peptide	^{99m}TC	SPECT/CT	BxPC-3	[66]
			Peptide	Phthalocyanine dye	NIRF imaging	BxPC-3	[67]
			Peptide	^{18}F-fluorobenzoate	PET	BxPC-3	[68]
CEA	Glycoprotein (immunoglobulin superfamily) [69]	Tumor cell migration, circulation, implantation and proliferation, which is facilitated by the immunosuppressive effect of CEA [70]	scFv	800CW	NIRF imaging	BxPC-3	[71]
			MAB	IR700	NIRF imaging	BxPC-3	[72]
			MAB	AlexaFluor 488	NIRF imaging	BxPC-3	[73–77]
			scFv	I^{124}	PET/CT	BxPC-3	[78]
cMET	Tyrosine kinase receptor (HGFR family) [79]	Tumor cell proliferation, survival, motility, and invasion [79]	–	–	–	–	–
EGFR	Tyrosine kinase receptor (ErbB family) [80]	Induces tumor cell differentiation and proliferation [81]	$F(ab')_2$ fragments [82]		^{64}Cu	PET/CT	PANC-1
			MAB	CF-750	MSOT	MiaPaCa-2	[83]
			scFv	IONP	MRI	MiaPaCa-2	[84, 85]
	XIMAB	^{86}Y	PET	SHAW	[86]		
	EpCAM	Transmembrane glycoprotein [87]	Tumor cell	proliferation, migration, and mitogenic signal transduction [87]	–	–	–
–	–						
HER2	Tyrosine kinase receptor (ErbB family) [88]	Tumor cell proliferation, survival, adhesion, and migration [88]	MAB	^{111}In	PET	PC-Sw	[89]
uPAR	GPI-anchored receptor (plasminogen activation system) [71]	Tumor cell migration, proliferation, and survival [90]	ATF-uPA	NIR-830, IONP	NIRF imaging, MRI	MiaPaCa-2	[84, 91–93]
			MAB	Cy5.5	NIRF imaging	AsPC-1	[94]
	VEGFR2	Tyrosine kinases receptor (VEGFR family) [95]		Angiogenesis during tumorgenesis [95]	MAB	Microbubbles	US
	Transgenic mouse model	[96–98]					

ATF amino terminal fragement, *CT* computed tomography, *FDA* Food and Drug Administration, *HGFR* hepatocyte growth factor receptor, *MAB* monoclonal antibody, *MPIO* microparticles of iron oxide, *MSOT* multispectral optoacoustic tomography *NIRF* near-infrared fluorescence, *NPIO* nanoparticles of iron oxide, *PC* pancreatic cancer, *PET* positron emission tomography, *scFv* single-chain antibody fragments, *SPECT* single-photon emission computed tomography, *uPA* urokinase plasminogen activator, *US* ultrasound, *VEGF* vascular endothelial growth factor, *VEGFR* vascular endothelial growth factor receptor, *XIMAB* chimeric human-mouse antibodies

5-µm sections were sliced. The sections were deparaffined in xylene and rehydrated in serially diluted alcohol solutions, followed by demineralized water according to standard protocols. Endogenous peroxidase was blocked by incubation in 0.3 % hydrogen peroxide in phosphate-buffered saline (PBS) for 20 min. For EpCAM, c-MET, HER2, and uPAR staining antigen retrieval was performed by heat induction at 95 °C using PT Link (Dako, Glostrup, Denmark) with a low-pH Envision FLEX target retrieval solution (citrate buffer pH 6.0, Dako). VEGFR staining required antigen retrieval with high-pH Envision FLEX target retrieval solution

(Tris-EDTA pH 9.0, Dako). For staining of EGFR and integrin $\alpha_v\beta_6$, antigen retrieval was performed with 0.4 % pepsin incubation for 10 min at 37 °C. CEA staining did not require antigen retrieval. Immunohistochemical staining was performed by incubating tissue microarrays overnight with antibodies against VEGFR2 (55B11; Cell Signaling Technology, Danvers, MA, USA), EpCAM (323A3, in-house produced hybridoma), c-MET (SC10; Santa Cruz Biotechnology, Santa Cruz, CA, USA), CEA (A0155; Dako, Glustrup, Denmark), EGFR (E30; Dako), integrin $\alpha_v\beta_6$ (6.2A; Biogen Idec MA Inc., Cambridge, MA, USA), HER2 (A0485; Dako), and uPAR (ATN-615, kindly provided by Prof A.P. Mazar, Northwestern University, Evanston, IL) all at room temperature [22, 23]. All antibodies were used at predetermined optimal dilutions using proper positive and negative control tissue. Furthermore, all antibodies selected for this study were solely selective for integrin $\alpha_v\beta_6$, CEA, cMET, EGFR, EpCAM, HER2, uPAR, and VEGFR respectively, except for the CEA antibody (A0155; Dako) that was also sensitive to CEA-like proteins (CEACAM1, CEACAM3, CEACAM4, CEACAM 6, CEACAM7, CEACAM 8) and the uPAR antibody (ATN-615) that also recognizes the soluble form of uPAR suPAR [22]. Negative control samples were incubated with PBS instead of the primary antibodies. The sections were washed with PBS, followed by incubation with Envision anti-mouse (K4001; Dako) or Envision anti-Rabbit (K4003; Dako), where applicable, for 30 min at room temperature. After additional washing, immunohistochemical staining was visualized using 3,3-diaminobenzidine tertahydrochloride solution (Dako) for 5–10 min resulting in brown color and counterstained with hematoxylin, dehydrated, and finally mounted in pertex. All stained sections were scanned and viewed at ×40 magnification using the Philips Ultra Fast Scanner 1.6 RA (Philips, Eindhoven, Netherlands). The numerical value for overall intensity (intensity score) was based on a four-point system: 0, 1, 2, and 3 (for none, light, medium, or high intense staining), as previously described by Choudhury et al., and staining was considered positive if >10 % of the tumor cells expressed a medium or dark staining pattern [23–29]. Evaluation of the immunohistochemical staining of all molecular targets was performed blinded and independently by two observers (S.W.L.G. and H.A.J.M.P). In case of disagreement, the stainings were discussed until agreement was reached.

Target Selection Criteria

The TASC score is based on granting points for the following seven characteristics of suitable molecular targets: extracellular protein localization (receptor bound to cell surface, 5 points; in close proximity of the tumor cell, 3 points); diffuse upregulation through tumor tissue (4 points); tumor-to-healthy cell (T/N) ratio (T/N ratio >10, 3 points); high percentage upregulation in patients (>90 %, 6 points; 70–90 %, 5 points; 50–69 %, 3 points; 10–49 %, 0 points); previous imaging success *in vivo* (2 points); enzymatic activity (1 point); and target-mediated internalization (1 point). All biomarkers were granted points for the seven characteristics and a total score of 18 or higher indicated that the biomarker is potentially suitable for tumor-targeted imaging *in vivo* [17]. Whereas a T/N ratio could not be obtained from immunohistochemical staining, we simplified the T/N ratio to a significant lower staining intensity in normal pancreatic tissue compared to pancreatic and periampullary adenocarcinoma. For the purpose of this study, diffuse expression was defined as staining in ≥50 % of tumor cells in the majority (>50 %) of the patients; focal expression as staining in <50 % of tumor cells in the majority (>50 %) of the patients and negative expression as staining in 0 % of the tumor cells in the majority (>50 %) of the patients.

Statistical Analysis

The statistical analysis was performed using SPSS version 23.0 software (SPSS, © IBM Corporation, Somer NY, USA) and GraphPad Prism 6 (GraphPad, Software, Inc., La Jolla, CA, USA). Interobserver variation of immunohistochemical results was analyzed using Cohen's kappa coefficient, and >0.8 was considered as acceptable. Baseline characteristics between groups were analyzed using chi-squared test for categorical data. Immunohistochemistry staining intensity in normal pancreatic tissue was compared to pancreatic and periampullary adenocarcinoma using the independent Student's t test. In all tests, results were considered statistically significant at the level of $p < 0.05$.

Results

Patient and Tumor Characteristics

In total, 165 patients were included, whereof 137 and 28 with pancreatic and periampullary adenocarcinoma, respectively (Table 2). The mean age was 66 years and ranged between 38 and 84 years. Most tumors were T-stage 3 (50.9 %) and poorly differentiated (44.6 %). Regional lymph node involvement was found in 69.7 % of patients. The majority of the patients received no adjuvant therapy after surgery. Patients diagnosed with adenocarcinoma originating from the pancreas had, compared to patients diagnosed with periampullary adenocarcinoma, more frequently lymph node invasion (75 vs. 43 %; $p < 0.001$), positive surgical margins (31 vs. 11 %; $p = 0.037$), vascular invasion (33 vs. 11 %; $p = 0.023$), perineural invasion (64 vs. 37 %; $p = 0.011$),

Table 2. Baseline characteristics for the patients with pancreatic and periampullary adenocarcinoma included in this study

Characteristics	Total population (n = 165)	Pancreatic adenocarcinoma (n = 137)	Periampullary adenocarcinoma (n = 28)	p-value
Age, *n* (%)				
<65 years	76 (46.1 %)	66 (48.2 %)	10 (35.6 %)	0.228
≥65 years	89 (53.9 %)	71 (51.8 %)	18 (64.3 %)	
Gender, *n* (%)				
Male	80 (48.5 %)	66 (48.2 %)	14 (50.0 %)	0.860
Female	85 (51.5 %)	71 (51.8 %)	14 (50.0 %)	
Tumor location, *n* (%)				
Pancreatic head	155 (93.9 %)	127 (92.7 %)	28 (100.0 %)	–
Other	10 (6.1 %)	10 (7.3 %)	–	
Tumor differentiation, *n* (%)				
Well differentiated	17 (13.3 %)	12 (8.8 %)	5 (17.9 %)	0.224
Moderately differentiated	54 (42.2 %)	43 (31.4 %)	11 (39.3 %)	
Poorly/undifferentiated	57 (44.6 %)	45 (32.8 %)	12 (42.8 %)	
Missing	37	37	–	
Tumor size, *n* (%)				
<30 mm	97 (59.9 %)	77 (57.5 %)	20 (71.4 %)	0.170
≥30 mm	65 (40.1 %)	57 (42.5 %)	8 (28.6 %)	
Missing	3	3	–	
Primary tumor, *n* (%)				
pT1	31 (18.8 %)	21 (15.3 %)	10 (35.7 %)	0.071
pT2	40 (24.2 %)	36 (26.3 %)	4 (14.3 %)	
pT3	84 (50.9 %)	72 (52.6 %)	12 (42.9 %)	
pT4	10 (6.1 %)	8 (5.8 %)	2 (7.1 %)	
Regional lymph node, *n* (%)				
pN0	50 (30.3 %)	34 (24.8 %)	16 (57.1 %)	<0.001
pN1	115 (69.7 %)	103 (75.2 %)	12 (42.9 %)	
Surgical margin status, *n* (%)				
R0	119 (72.6 %)	95 (69.3 %)	24 (88.9 %)	0.037
R1	45 (27.4 %)	42 (30.7 %)	3 (11.1 %)	
Adjuvant therapy, *n* (%)				
Yes	70 (42.4 %)	68 (49.6 %)	2 (7.1 %)	<0.001
No	95 (57.6 %)	69 (50.4 %)	26 (92.9 %)	
Vascular invasion, *n* (%)				
Positive	48 (29.3 %)	45 (32.8 %)	3 (11.1 %)	0.023
Negative	116 (70.7 %)	92 (67.2 %)	24 (88.9 %)	
Perineural invasion, *n* (%)				
Positive	97 (59.1 %)	87 (63.5 %)	10 (37.0 %)	0.011
Negative	67 (40.9 %)	50 (36.5 %)	17 (63.0 %)	

*p Value was obtained for patients with pancreatic adenocarcinoma compared to periampullary adenocarcinoma patients, and $p < 0.05$ was considered significant

and received more often adjuvant therapy (50 vs. 7 %; $p < 0.001$).

Biomarker Expression

Of the 165 pancreatic and periampullary adenocarcinoma specimens collectively present on the TMA, 159 specimens (96 %) could successfully be microscopically quantified for integrin $\alpha_v\beta_6$ expression, 158 (96 %) for CEA, 159 (96 %) for cMET, 156 (95 %) for EGFR, 151 (92 %) for EpCAM, 152 (92 %) for HER2, 155 (94 %) for VEGFR2, and 152 (92 %) for uPAR. The missing cases were due to staining artifacts, excessive necrotic tissue, or unacceptable tissue loss during the staining procedure. The molecular markers showed mainly membranous and cytoplasmic immunoreactivity in pancreatic and periampullairy adenocarcinoma cells; CEA and uPAR also showed stromal immunoreactivity (Fig. 1). Diffuse membranous staining was found for integrin $\alpha_v\beta_6$, CEA, cMET, EGFR, HER2, and uPAR in pancreatic adenocarcinoma (Table 3) and integrin $\alpha_v\beta_6$, CEA, cMET, EGFR, EpCAM, HER2, and VEGFR2 in periampullary adenocarcinoma (Table 4). Immunohistochemistry staining, if present, in healthy pancreatic tissue was predominantly localized in the acinar cells of the pancreas. The most frequently expressed biomarkers were integrin $\alpha_v\beta_6$ and cMET that were both expressed in 88 % of the pancreatic adenocarcinoma cases (Table 3). In addition, cMET was abundantly expressed in 96 % of the periampullary adenocarcinoma patients (Table 4). To evaluate the ability of potential tumor-specific molecular markers to distinguish between pancreatic adenocarcinoma and healthy pancreatic tissue, the mean immunohistochemical intensity scores of the biomarkers were compared between both tissue types. In pancreatic adenocarcinoma, the mean intensity score for integrin $\alpha_v\beta_6$ ($p < 0.001$; $p < 0.001$), CEA ($p < 0.001$; $p < 0.001$),

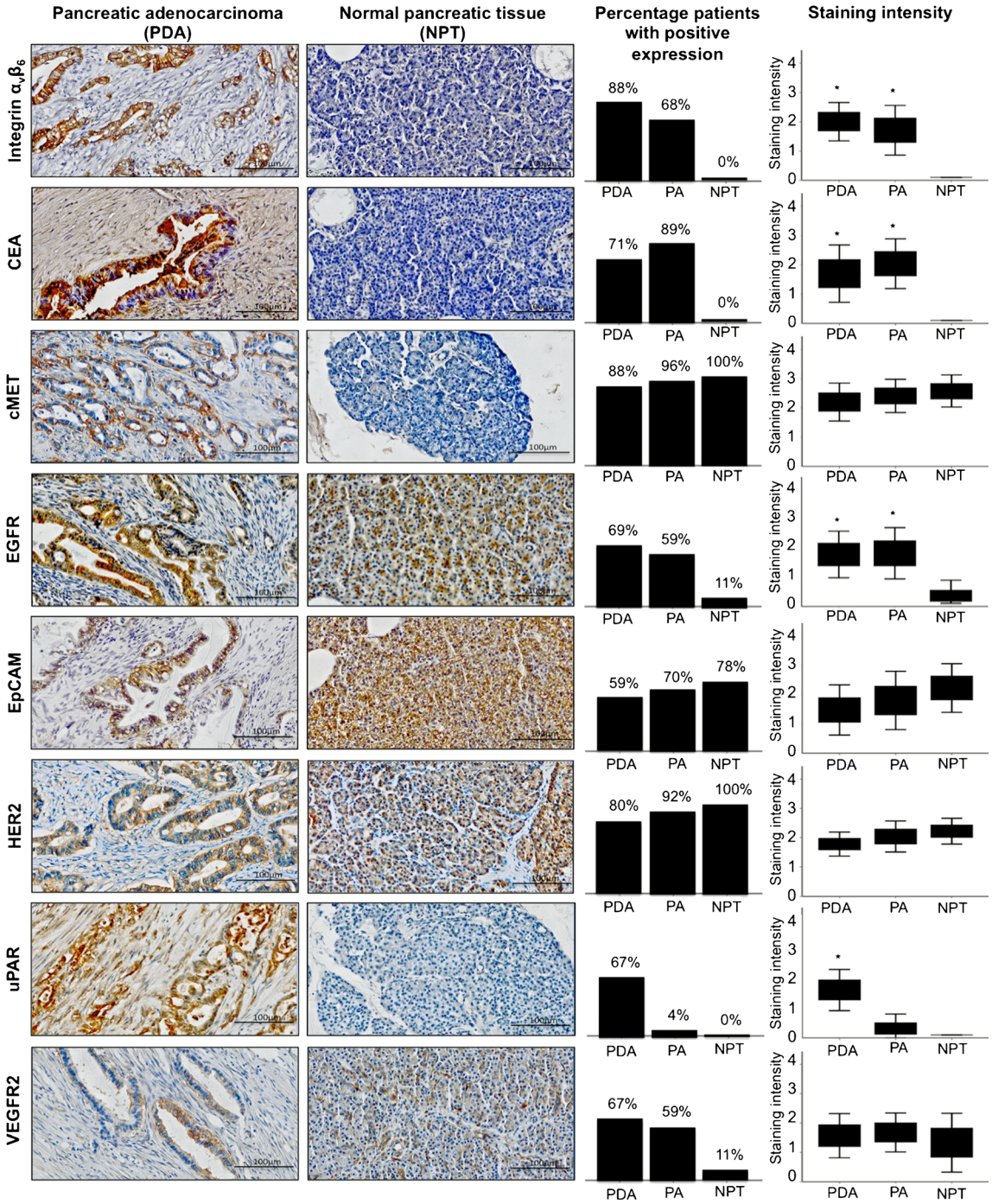

Fig. 1 Representative images of moderate immunohistochemistry staining in pancreatic adenocarcinoma (*left column*) and absent or present immunohistochemistry expression in pancreatic adenocarcinoma (*second left column*), followed by bar charts (*third left column*) displaying the percentage of PAC patients with positive staining (positive staining was defined as moderate or strong expression in >10 % of tumor cells) and boxplots (*right column*) showing the mean immunohistochemistry staining (staining intensity was classified for every patient as followed: 0 = negative, 1 = weak, 2 = moderate, and 3 = strong) in pancreatic adenocarcinoma (PDA), periampullary adenocarcinoma (PA), and normal pancreatic tissue (NPT) for integrin $\alpha_v\beta_6$, carcinoembryonic antigen (CEA), hepatocyte growth factor receptor (cMET), epithelial growth factor receptor (EGFR), epithelial cell adhesion molecule (EpCAM), human epithelial growth factor receptor (HER2), urokinase receptor (uPAR), and vascular endothelial growth factor receptor 2 (VEGFR2) expression. *Significant difference in staining intensity (defined as *p* value of 0.05) in pancreatic or periampullary adenocarcinoma compared to normal pancreatic tissue.

Table 3. Target Selection Criteria (TASC) score for integrin $\alpha_v\beta_6$, carcinoembryonic antigen (CEA), hepatocyte growth factor receptor (cMET), epithelial growth factor receptor (EGFR), epithelial cell adhesion molecule (EpCAM), human epidermal growth factor receptor (HER2), urokinase receptor (uPAR), and vascular endothelial growth factor receptor 2 (VEGFR2) in pancreatic adenocarcinoma

Target	Extracellular localization of the protein (points awarded)	Pattern of upregulation (points awarded)	T/N ratio (points awarded)	Percentage with positive expression (points awarded)	Previous imaging success (points awarded)	Enzymatic activity (points awarded)	Internalization (points awarded)	TASC Score
Integrin $\alpha_v\beta_6$	Membrane-bound (3) [99]	Diffuse (4)	Yes (3)	88 % (5)	Animal experiment (2) [68]	No (0) [100]	Yes (1) [65]	20
CEA	Membrane-bound (3) [101]	Diffuse (4)	Yes (3)	71 % (5)	Animal experiment (2) [74, 77]	Unknown (0)	Yes (1) [102]	20
UPAR	Membrane-bound (3) [71]	Diffuse (4)	Yes (3)	67% (3)	Animal experiment (2) [91]	Yes (1) [103]	Yes (1) [104]	19
cMET	Membrane-bound (3) [105]	Diffuse (4)	No (0)	88% (5)	Animal experiment (2) [106]	Yes (1) [107]	Yes (1) [108]	18
EGFR	Membrane-bound (3) [109]	Diffuse (4)	Yes (3)	69% (3)	In patients (2) [86, 110]	Unknown (0)	Yes (1) [111]	18
HER2	Membrane-bound (3) [112]	Diffuse (4)	No (0)	80% (5)	Animal experiment (2) [89]	Unknown (0)	Yes (1) [113]	17
VEGFR2	Membrane-bound (3) [114]	Focal (0)	No (0)	72% (5)	Animal experiment (2) [115]	Yes (1) [116]	Yes (1) [117]	14
EpCAM	Membrane-bound (3) [118]	Focal (0)	No (0)	59% (3)	Animal experiment (2) [119]	Unknown (0)	Yes (1) [120]	11

Extracellular localization of the protein was based on the literature; pattern of upregulation was obtained from the immunohistochemical staining (diffuse, staining in ≥50 % of tumor cells in the majority (>50 %) of the patients; focal, staining in <50 % of tumor cells in the majority (>50 %) of the patients; or negative, staining in 0 % of the tumor cells in the majority (>50 %) of the patients) described in this study; tumor to normal (T/N) ratio of the biomarker expression, as determined by significant higher mean immunohistochemistry staining (staining intensity was classified for every patient as follows: 0 = negative, 1 = weak, 2 = moderate, and 3 = strong) in pancreatic adenocarcinoma compared to normal pancreatic tissue; percentage of patients with positive expression were described according the findings of the current study; previous imaging success was defined as published *in vivo* tumor-specific imaging studies directed at the target; enzymatic activity refers to enzymatic activity of the target in and around the tumor described in the literature, that potentially can be used for locally activated probes; internalization indicates the receptor could have the ability to internalize the probe-target complex in the tumor cell according to previous studies

EGFR ($p<0.001$; $p<0.001$), and uPAR ($p<0.001$; $p=0.056$) was significantly higher compared to normal pancreatic tissue (Fig. 1). In periampullary adenocarcinoma, the mean integrin $\alpha_v\beta_6$ ($p<0.001$), CEA ($p<0.001$), and VEGFR2 ($p=0.045$) staining intensity were significantly higher.

Biomarker Panels

The combined expression of two biomarkers was evaluated to assess their potential as a dual target for tumor-specific imaging (Table 5). In pancreatic adenocarcinoma, integrin $\alpha_v\beta_6$ and/or CEA were expressed in 99 % of the patients and 64 % of the cases expressed both integrin $\alpha_v\beta_6$ and CEA, suggesting that the combination of both targets would be a promising approach for tumor-specific imaging. In periampullary adenocarcinoma, the most promising combination was CEA and EGFR, whereas all cases expressed either CEA and/or EGFR. In addition, integrin $\alpha_v\beta_6$ and/or CEA were expressed in 96 % of the cases.

TASC Score

The TASC score was calculated for all molecular markers evaluated in this study (Tables 3 and 4). Integrin $\alpha_v\beta_6$ (20 points), CEA (20 points), uPAR (19 points), cMET (18 points), and EGFR (18 points) were considered suitable targets for tumor-specific imaging of pancreatic adenocarcinoma according the TASC score. For tumor-specific imaging of periampullary adenocarcinoma, VEGFR2 (21 points), CEA (20 points), cMET (19 points), EGFR (18 points), and integrin $\alpha_v\beta_6$ (18 points) were categorized as potential targets by the TASC scoring system.

Discussion

Tumor-specific intraoperative imaging is a rapidly emerging field that holds great promise to reduce tumor-positive resection margin rates in oncologic pancreatic surgery [30]. However, to make the transition to clinical practice, tumor-specific imaging targets and accompanying contrast agents are prerequisite [15]. Therefore, the present study strives to provide the first steps toward clinical translation by investigating the suitability of a set of molecular markers

Table 4. Target Selection Criteria (TASC) score for integrin $\alpha_v\beta_6$, carcinoembryonic antigen (CEA), hepatocyte growth factor receptor (cMET), epithelial growth factor receptor (EGFR), epithelial cell adhesion molecule (EpCAM), human epidermal growth factor receptor (HER2), urokinase receptor (uPAR), and vascular endothelial growth factor receptor 2 (VEGFR2) in periampullary adenocarcinoma

Target	Extracellular protein localization of the protein (points awarded)	Pattern of upregulation (points awarded)	T/N ratio (points awarded)	Percentage with positive expression (points awarded)	Previously imaged (points awarded)	Enzymatic activity (points awarded)	internalization (points awarded)	TASC Score
VEGFR2	Membrane-bound (3) [114]	Diffuse (4)	Yes (3)	86% (5)	Animal		experiment (2) [115]	Yes (1)
[116]	Yes (1) [117]	21						
CEA	Membrane-bound (3) [101]	Diffuse (4)	Yes (3)	89% (5)	Animal		experiment (2) [74, 77]	
	Unknown (0)	Yes (1) [102]	20					
cMET	Membrane-bound (3) [105]	Diffuse (4)	No (0)	96% (6)	Animal		experiment (2) [106]	Yes (1)
[107]	Yes (1) [108]	19						
EGFR	Membrane-bound (3) [109]	Diffuse (4)	Yes (3)	59% (3)	In patients (0) [86, 110]	Unknown (0)	Yes (1) [111]	18
Integrin $\alpha_v\beta_6$	Membrane-bound (3) [99]	Diffuse (4)	Yes (3)	68% (3)	Animal		experiment (2) [68]	No (0)
[100]	Yes (1) [65]	18						
EpCAM	Membrane-bound (3) [118]	Diffuse (4)	No (0)	68% (3)	Animal		experiment (2) [119]	
	Unknown (0	Yes (1) [120]	17					
HER2	Membrane-bound (3) [112]	Diffuse (4)	No (0)	88% (5)	Animal		experiment (2) [89]	
	Unknown (0	Yes (1) [113]	17					
UPAR	Membrane-bound (3) [71]	Focal (0)	Yes (3)	4% (0)	Animal		experiment (2) [91]	Yes (1)
[103]	Yes (1) [104]	12						

Extracellular localization of the protein was based on the literature; pattern of upregulation was obtained from the immunohistochemical staining (diffuse, staining in ≥50 % of tumor cells in the majority (>50 %) of the patients; focal, staining in <50 % of tumor cells in the majority (>50 %) of the patients; or negative, staining in 0 % of the tumor cells in the majority (>50 %) of the patients) described in this study; tumor to normal (T/N) ratio of the biomarker expression, as determined by significant higher mean immunohistochemistry staining (staining intensity was classified for every patient as follows: 0 = negative, 1 = weak, 2 = moderate, and 3 = strong) in periampullary adenocarcinoma compared to normal pancreatic tissue; percentage of patients with positive expression; percentage of patients with positive expression were described according the findings of the current study; previous imaging success was defined as published *in vivo* tumor-specific imaging studies directed at the target; enzymatic activity refers to enzymatic activity of the target in and around the tumor described in the literature, that potentially can be used for locally activated probes; internalization indicates the receptor could have the ability to internalize the probe-target complex in the tumor cell according to previous studies

as potential targets for tumor-specific imaging of pancreatic adenocarcinoma. The results of this study show that integrin $\alpha_v\beta_6$, CEA, EGFR, and uPAR are significantly upregulated in pancreatic adenocarcinoma compared to healthy pancreatic tissue and suggest that these biomarkers are promising targets for tumor-specific contrast agent development. By combining individual biomarkers in dual biomarker panels, the coverage of patients was increased: in pancreatic adenocarcinoma, considering almost the complete population expressed either integrin $\alpha_v\beta_6$ and/or CEA. Furthermore,

Table 5. Expression, as determined by immunohistochemistry, of biomarkers panels (combining the expression of two molecular markers) consisting of integrin $\alpha_v\beta_6$, carcinoembryonic antigen (CEA), epithelial growth factor receptor (EGFR), and/or urokinase receptor (uPAR) in pancreatic and periampullary adenocarcinoma

Biomarker panel		Total population		Pancreatic adenocarcinoma		Periampullary adenocarcinoma	
		Overlapping expression	Total expression	Overlapping expression	Total expression	Overlapping expression	Total expression
Integrin $\alpha_v\beta_6$	CEA	64 %	97 %	64 %	99 %	63 %	96 %
Integrin $\alpha_v\beta_6$	uPAR	52 %	90 %	62 %	96 %	4 %	73 %
Integrin $\alpha_v\beta_6$	EGFR	62 %	91 %	66 %	94 %	44 %	82 %
CEA	uPAR	43 %	91 %	50 %	91 %	4 %	88 %
CEA	EGFR	52 %	91 %	52 %	90 %	54 %	100 %
uPAR	EGFR	40 %	83 %	48 %	88 %	60 %	68 %

Overlapping expression refers to the percentage of patients that show positive expression (positive expression was defined as positive if >10 % of the tumor cells expressed a moderate or strong staining pattern) for both molecular markers in the biomarker panel. Total expression describes the frequency of patients that show positive expression (positive expression was defined as positive if >10 % of the tumor cells expressed a moderate or strong staining pattern) of one or both molecular markers in the biomarker panel and therefore could be visualized with a dual-tracer targeting both biomarkers

the TASC score confirmed the potential of integrin $\alpha_v\beta_6$, CEA, EGFR, and uPAR as suitable targets for tumor-specific imaging.

Previous reports regarding the expression of integrin $\alpha_v\beta_6$ (85–100 %), cMET (82–100 %), EGFR (36–69 %), EpCAM (56–78 %), HER2 (16–69 %), and VEGFR2 (64–93 %) in pancreatic adenocarcinoma are consistent with our results [31–47]. Preceding findings demonstrate a higher expression of CEA (98–100 %) and uPAR (90–96 %) in pancreatic adenocarcinoma to our findings; however, this slight discrepancy is not likely to alter the final conclusion of this study [33, 35, 48]. Furthermore, studies of others showed analogue to our results that cMET, EpCAM, and HER2 are overexpressed in healthy pancreatic tissue, which would render them less preferable as imaging targets [37, 38, 40–42]. Importantly, the expression of integrin $\alpha_v\beta_6$, CEA, and uPAR has been described previously in compliance with our results, as very low or undetectable in normal pancreatic tissue, which would translate to a favorable tumor-to-background ratio when used for imaging purposes [31, 35, 48, 49]. EGFR and VEGFR2 were previously shown as respectively present and absent in normal pancreatic tissue, contradicting our findings [41, 42, 49]. This ambiguity highlights the need to further investigate the ability of EGFR and VEGFR to distinguish between normal and malignant pancreatic tissue, especially since fluorescence-labeled contrast agents directed at EGFR and VEGF, including bevacizumab-IRDye800CW, cetuximab-IRDye800CW, and panitumab-IRDye800CW, are in various stages of clinical trials for clinical use in several other types of cancer [15].

The results of this study are posed by limitations inherent to immunohistochemical analysis, such as variation in the quality of the primary antibodies, immunohistochemical staining techniques, scoring criteria, paraffin impregnation, surgical specimen fixation delay, or diversity in the ethnic distribution of the study population [50, 51]. In addition, the immunohistochemistry procedure, including tissue fixation and antigen retrieval, destroys the membrane integrity and protein conformation, which makes the protein less representative for its naive counterpart. The antibodies used in this study were not specifically selected for the development of tumor-specific probes, since the focus of this study was to identify the most suitable targets; however, the antibodies in this study used for integrin $\alpha_v\beta_6$ (6.2A, Biogen Idec MA Inc.), CEA (A0155, Dako), EGFR (E30, Dako), EpCAM (323A3), and uPAR (ATN-615) react on the extracellular epitopes of their analogues and have been described for use on intact protein [52]. The latter could be promising for use in imaging probes. Furthermore, the normal pancreatic tissue used in this study was obtained in proximity of the tumor for an optimal representation of the reality of image-guided surgery. Premalignant biological changes may already exist in this presumed normal pancreatic tissue, which could explain for the differences between our findings and the biomarker expression in normal pancreatic tissue reported in the literature. For the purpose of this study, the term periampullary adenocarcinoma was used as an omnibus term for a very a heterogeneous group of adenocarcinoma that invade the head of the pancreas with distinctively different histology and expression of molecular markers as they originate from the duodenum, papilla of Vateri or the common bile duct. Hence, it is challenging or even impossible to draw conclusions that are true for the whole cohort periampullary adenocarcinoma based on our findings or represent them with a histology slide in Fig. 1. Moreover, this study applies a threshold of over 10 % medium or dark stained tumor cells on 2-mm core TMAs to define tumor positivity. Therefore, the results of this study do not provide conclusive evidence on whether the evaluated targets could be used for tumor-specific imaging of the complete tumor and all residual disease. Nevertheless, the results of this study provide guidance on which molecular makers show the most promise for further investigation as tumor-specific imaging targets. Likewise, the reported expression of the composed biomarker panels investigated in this study indicates which biomarker combinations show complementary instead of overlapping expression in the majority of pancreatic adenocarcinoma and subsequently holds promise for future more elaborate examination. However, considering the >10 % threshold, these results are not decisive on whether dual tracers directed at the inquired biomarker panels will be able to visualize the entire disease burden.

The TASC score identified cMET as a promising imaging target for pancreatic adenocarcinoma, whereas cMET did not significantly differentiate between healthy and malignant pancreatic tissue in our hands. These results suggest that the TASC score still experiences teething trouble and needs further validation and adaptation, since distinguishing between normal and malignant tissue is considered the cornerstone of surgical oncology. Various therapeutic antibodies have been investigated in preclinical models for imaging of cancer, including cetuximab, panitumumab, and bevacizumab [53–56]. Human clinical trials are underway, but none of these biologics are presently available for intraoperative imaging in humans. Use of an FDA-approved targeting molecule facilitates clinical translation, because it lowers the cost barrier to clinical practice, since revenue associated with diagnostic agents is significantly lower than for therapeutic agents [16, 57]. Therefore, for future use, the TASC score should also take into consideration the availability of FDA-approved antibodies. Nevertheless, de novo development of intraoperative diagnostics also takes place, for example, the Arg-Gly-Asp (RGD) peptide has a high affinity and selectivity for multiple integrins, among them integrin $\alpha_v\beta_6$, and has extensively been studied for imaging objectives [58, 59]. In addition, another example of *de novo* developed imaging probes are autoquenched fluorescent probes, such as ProSense, that convert from a

nonfluorescent to fluorescent state by proteolytic activation of lysosomal cysteine or serine proteases, hence the value of including enzymatic activity in by the TASC score [60]. Furthermore, the TASC criteria could be elaborated by adding points to the score for targets with a soluble form that can be targeted by certain antibodies, such as the ATN-615 antibody that recognizes a soluble form of uPA in addition to uPAR, which allows for antibodies to also target receptors that are already occupied by its soluble form thereby increasing its reach. Nevertheless, the TASC score is a promising tool to incorporate other favorable characteristics of potential imaging targets for pancreatic adenocarcinoma in a weighted and standardized manner in our judgment.

Despite the previously mentioned limitations, this study was to the best of our knowledge the first study to assess the ability of potential targets for the image-guided surgery of pancreatic adenocarcinoma to distinguish between normal and malignant pancreatic tissue in a relatively large cohort of patients with pancreatic adenocarcinoma using the TASC score. In addition, this study was also able to investigate the expression of potential imaging targets in periampullary adenocarcinoma. The latter is of added value since the histological origin of pancreatic head masses is often unknown in wait of pancreatic surgery. Furthermore, this study was to our knowledge the first to describe the combined expression of potential imaging targets to facilitate future development of dual-labeled imaging probes; however, these dual-purpose agents present additional hurdles in development and clinical translation that are beyond the scope of this article before their potential is fully realized [16]. Moreover, aside from providing guidance for tumor surgery, molecular imaging techniques also play an increasingly important role in the preoperative staging and guidance of cancer therapy in pancreatic adenocarcinoma patients [61].

In conclusion, tumor-targeted intraoperative imaging of pancreatic adenocarcinoma has great potential to improve pancreatic surgery [12, 62]. However, the clinical implementation of this novel technique is currently halted by the lack of clinically approved tumor-specific contrast agents. Therefore, the present study sought to pave the way for future development of tumor-specific contrast agents and consecutive image-guided resection of pancreatic adenocarcinoma, by investigating the most suitable molecular targets for tumor-specific imaging. The results of this study show that a dual-targeted tracer aimed at both integrin $\alpha_v\beta_6$ and CEA would be able to detect tumor cells in 99 % of all pancreatic cancer patients.

Acknowledgments. The authors kindly thank A.P. Mazar from the Northwestern University (Evanston, USA) for providing the anti-uPAR (ATN-615) antibodies and R. Keijzer, R. Vlierberghe, N.G. Dekker-Ensink, and C.M. Janssen for their technical expertise in the field of immunohistochemistry. This work was supported by the project grant H2020-MSCA-RISE grant number 644373–PRISAR (P.J.K. Kuppen), the Center for Translational Molecular Medicine project grant 03O-202 (A.L. Vahrmeijer), the Dutch Cancer Society grant UL2010-4732 (A.L. Vahrmeijer), and the Dutch Cancer Association Bas Mulder Award (J.S.D. Mieog).

Compliance with Ethical Standards

Conflict of Interest

The authors declare that they have no conflict of interest.

References

1. Siegel R, Ma J, Zou Z, Jemal A (2014) Cancer statistics, 2014. CA Cancer J Clin 64:9–29
2. Cameron JL, Crist DW, Sitzmann JV et al (1991) Factors influencing survival after pancreaticoduodenectomy for pancreatic cancer. Am J Surg 161:120–125
3. Qiao QL, Zhao YG, Ye ML et al (2007) Carcinoma of the ampulla of Vater: factors influencing long-term survival of 127 patients with resection. World J Surg 31:137–143, discussion 144-136
4. Tummala P, Howard T, Agarwal B (2013) Dramatic survival benefit related to R0 resection of pancreatic adenocarcinoma in patients with tumor </=25 mm in size and </=1 involved lymph nodes. Clin Transl Gastroenterol 4:e33
5. Merkow RP, Bilimoria KY, Bentrem DJ et al (2014) National assessment of margin status as a quality indicator after pancreatic cancer surgery. Ann Surg Oncol 21:1067–1074
6. Chang DK, Johns AL, Merrett ND et al (2009) Margin clearance and outcome in resected pancreatic cancer. J Clin Oncol 27:2855–2862
7. Esposito I, Kleeff J, Bergmann F et al (2008) Most pancreatic cancer resections are R1 resections. Ann Surg Oncol 15:1651–1660
8. Neoptolemos JP, Dunn JA, Stocken DD et al (2001) Adjuvant chemoradiotherapy and chemotherapy in resectable pancreatic cancer: a randomised controlled trial. Lancet 358:1576–1585
9. Appel BL, Tolat P, Evans DB, Tsai S (2012) Current staging systems for pancreatic cancer. Cancer J 18:539–549
10. Handgraaf HJ, Boonstra MC, Van Erkel AR et al (2014) Current and future intraoperative imaging strategies to increase radical resection rates in pancreatic cancer surgery. Biomed Res Int 2014:890230
11. van Dam GM, Themelis G, Crane LM et al (2011) Intraoperative tumor-specific fluorescence imaging in ovarian cancer by folate receptor-alpha targeting: first in-human results. Nat Med 17:1315–1319
12. Vahrmeijer AL, Hutteman M, van der Vorst JR, van de Velde CJ, Frangioni JV (2013) Image-guided cancer surgery using near-infrared fluorescence. Nat Rev Clin Oncol 10:507–518
13. Vahrmeijer AL, Frangioni JV (2011) Seeing the invisible during surgery. Br J Surg 98:749–750
14. Stummer W, Pichlmeier U, Meinel T et al (2006) Fluorescence-guided surgery with 5-aminolevulinic acid for resection of malignant glioma: a randomised controlled multicentre phase III trial. Lancet Oncol 7:392–401
15. Rosenthal EL, Warram JM, de Boer E, et al. (2015) Successful translation of fluorescence navigation during oncologic surgery: a consensus report. J Nucl Med 57:144–50
16. Rosenthal EL, Warram JM, Bland KI, Zinn KR (2015) The status of contemporary image-guided modalities in oncologic surgery. Ann Surg 261:46–55
17. van Oosten M, Crane LM, Bart J et al (2011) Selecting potential targetable biomarkers for imaging purposes in colorectal cancer using TArget Selection Criteria (TASC): a novel target identification tool. Transl Oncol 4:71–82
18. Pomianowska E, Grzyb K, Westgaard A et al (2012) Reclassification of tumour origin in resected periampullary adenocarcinomas reveals underestimation of distal bile duct cancer. Eur J Surg Oncol 38:1043–1050
19. Yeo CJ, Cameron JL, Lillemoe KD et al (2002) Pancreaticoduodenectomy with or without distal gastrectomy and extended retroperitoneal lymphadenectomy for periampullary adenocarcinoma, part 2: randomized controlled trial evaluating survival, morbidity, and mortality. Ann Surg 236:355–366, discussion 366-358
20. Mizukami T, Kamachi H, Mitsuhashi T et al (2014) Immunohistochemical analysis of cancer stem cell markers in pancreatic adenocarcinoma patients after neoadjuvant chemoradiotherapy. BMC Cancer 14:687

21. Greene FLP, Page DL, Flemming ID, Fritz A, Balch CM, Haller DG, Monica M (2002) American joint committee on cancer: AJCC cancer staging manual, 6th edn. Springer, New York
22. Li Y, Parry G, Chen L et al (2007) An anti-urokinase plasminogen activator receptor (uPAR) antibody: crystal structure and binding epitope. J Mol Biol 365:1117–1129
23. Hildenbrand R, Niedergethmann M, Marx A et al (2009) Amplification of the urokinase-type plasminogen activator receptor (uPAR) gene in ductal pancreatic carcinomas identifies a clinically high-risk group. Am J Pathol 174:2246–2253
24. Niu Z, Wang J, Muhammad S et al (2014) Protein expression of eIF4E and integrin alphavbeta6 in colon cancer can predict clinical significance, reveal their correlation and imply possible mechanism of interaction. Cell Biosci 4:23
25. He MM, Zhang DS, Wang F et al (2014) Adjuvant chemotherapy, p53, carcinoembryonic antigen expression and prognosis after D2 gastrectomy for gastric adenocarcinoma. World J Gastroenterol 20:264–273
26. de Melo MB, Fontes AM, Lavorato-Rocha AM et al (2014) EGFR expression in vulvar cancer: clinical implications and tumor heterogeneity. Hum Pathol 45:917–925
27. Zorgetto VA, Silveira GG, Oliveira-Costa JP et al (2013) The relationship between lymphatic vascular density and vascular endothelial growth factor A (VEGF-A) expression with clinical-pathological features and survival in pancreatic adenocarcinomas. Diagn Pathol 8:170
28. Kawamoto T, Ishige K, Thomas M et al (2014) Overexpression and gene amplification of EGFR, HER2, and HER3 in biliary tract carcinomas, and the possibility for therapy with the HER2-targeting antibody pertuzumab. J Gastroenterol 50:467–479
29. Choudhury KR, Yagle KJ, Swanson PE et al (2010) A robust automated measure of average antibody staining in immunohistochemistry images. J Histochem Cytochem 58:95–107
30. Metildi CA, Kaushal S, Hardamon CR et al (2012) Fluorescence-guided surgery allows for more complete resection of pancreatic cancer, resulting in longer disease-free survival compared with standard surgery in orthotopic mouse models. J Am Coll Surg 215:126–135, discussion 135-126
31. Sipos B, Hahn D, Carceller A et al (2004) Immunohistochemical screening for beta6-integrin subunit expression in adenocarcinomas using a novel monoclonal antibody reveals strong up-regulation in pancreatic ductal adenocarcinomas *in vivo* and *in vitro*. Histopathology 45:226–236
32. Zhu GH, Huang C, Qiu ZJ et al (2011) Expression and prognostic significance of CD151, c-Met, and integrin alpha3/alpha6 in pancreatic ductal adenocarcinoma. Dig Dis Sci 56:1090–1098
33. Yamaguchi K, Enjoji M, Tsuneyoshi M (1991) Pancreatoduodenal carcinoma: a clinicopathologic study of 304 patients and immunohistochemical observation for CEA and CA19-9. J Surg Oncol 47:148–154
34. Moore TL, Kupchik HZ, Marcon N, Zamcheck N (1971) Carcinoembryonic antigen assay in cancer of the colon and pancreas and other digestive tract disorders. Am J Dig Dis 16:1–7
35. Allum WH, Stokes HJ, Macdonald F, Fielding JW (1986) Demonstration of carcinoembryonic antigen (CEA) expression in normal, chronically inflamed, and malignant pancreatic tissue by immunohistochemistry. J Clin Pathol 39:610–614
36. Neuzillet C, Couvelard A, Tijeras-Raballand A et al (2015) High c-Met expression in stage I-II pancreatic adenocarcinoma: proposal for an immunostaining scoring method and correlation with poor prognosis. Histopathology 67:664–76
37. Kiehne K, Herzig KH, Folsch UR (1997) c-met expression in pancreatic cancer and effects of hepatocyte growth factor on pancreatic cancer cell growth. Pancreas 15:35–40
38. Di Renzo MF, Poulsom R, Olivero M et al (1995) Expression of the Met/hepatocyte growth factor receptor in human pancreatic cancer. Cancer Res 55:1129–1138
39. Handra-Luca A, Hammel P, Sauvanet A et al (2014) EGFR expression in pancreatic adenocarcinoma. Relationship to tumour morphology and cell adhesion proteins. J Clin Pathol 67:295–300
40. Yamanaka Y, Friess H, Kobrin MS et al (1993) Overexpression of HER2/neu oncogene in human pancreatic carcinoma. Hum Pathol 24:1127–1134
41. Lemoine NR, Hughes CM, Barton CM et al (1992) The epidermal growth factor receptor in human pancreatic cancer. J Pathol 166:7–12
42. Korc M, Chandrasekar B, Yamanaka Y et al (1992) Overexpression of the epidermal growth factor receptor in human pancreatic cancer is associated with concomitant increases in the levels of epidermal growth factor and transforming growth factor alpha. J Clin Invest 90:1352–1360
43. Went PTH, Lugli A, Meier S et al (2004) Frequent EpCam protein expression in human carcinomas. Hum Pathol 35:122–128
44. Komoto M, Nakata B, Amano R et al (2009) HER2 overexpression correlates with survival after curative resection of pancreatic cancer. Cancer Sci 100:1243–1247
45. Yamanaka Y (1992) The immunohistochemical expressions of epidermal growth factors, epidermal growth factor receptors and c-erbB-2 oncoprotein in human pancreatic cancer. J Nippon Med Sch 59:51–61
46. Fong D, Steurer M, Obrist P et al (2008) Ep-CAM expression in pancreatic and ampullary carcinomas: frequency and prognostic relevance. J Clin Pathol 61:31–35
47. Day JH, Digiuseppe JA, Yeo C et al (1996) Immunohisatochemical Evaluation of HER2/neu expression in Pancreatic Adenocarcinoma and Pancreatic Intraepithelial Neoplasms. Hum Pathol 27:5
48. Cantero D, Friess H, Deflorin J et al (1997) Enhanced expression of urokinase plasminogen activator and its receptor in pancreatic carcinoma. Br J Cancer 75:388–395
49. Itakura J, Ishiwata T, Friess H et al (1997) Enhanced expression of vascular endothelial growth factor in human pancreatic cancer correlates with local disease progression. Clin Cancer Res 3:1309–1316
50. Blok EJ, Kuppen PJ, van Leeuwen JE, Sier CF (2013) Cytoplasmic overexpression of HER2: a key factor in colorectal cancer. Clin Med Insights Oncol 7:41–51
51. True LD (2014) Methodological requirements for valid tissue-based biomarker studies that can be used in clinical practice. Virchows Arch 464:257–263
52. Van Aarsen LA, Leone DR, Ho S et al (2008) Antibody-mediated blockade of integrin alpha v beta 6 inhibits tumor progression *in vivo* by a transforming growth factor-beta-regulated mechanism. Cancer Res 68:561–570
53. Day KE, Sweeny L, Kulbersh B et al (2013) Preclinical comparison of near-infrared-labeled cetuximab and panitumumab for optical imaging of head and neck squamous cell carcinoma. Mol Imaging Biol 15:722–729
54. Day KE, Beck LN, Deep NL et al (2013) Fluorescently labeled therapeutic antibodies for detection of microscopic melanoma. Laryngoscope 123:2681–2689
55. Heath CH, Deep NL, Beck LN et al (2013) Use of panitumumab-IRDye800 to image cutaneous head and neck cancer in mice. Otolaryngol Head Neck Surg 148:982–990
56. Day KE, Beck LN, Heath CH et al (2013) Identification of the optimal therapeutic antibody for fluorescent imaging of cutaneous squamous cell carcinoma. Cancer Biol Ther 14:271–277
57. Keereweer S, Kerrebijn JD, van Driel PB et al (2011) Optical image-guided surgery—where do we stand? Mol Imaging Biol 13:199–207
58. Plow EF, Haas TA, Zhang L et al (2000) Ligand binding to integrins. J Biol Chem 275:21785–21788
59. Chen H, Niu G, Wu H, Chen X (2016) Clinical application of radiolabeled RGD peptides for PET imaging of integrin alphavbeta3. Theranostics 6:78–92
60. Mieog JS, Vahrmeijer AL, Hutteman M et al (2010) Novel intraoperative near-infrared fluorescence camera system for optical image-guided cancer surgery. Mol Imaging 9:223–231
61. Haedicke K, Grafe S, Lehmann F, Hilger I (2013) Multiplexed *in vivo* fluorescence optical imaging of the therapeutic efficacy of photodynamic therapy. Biomaterials 34:10075–10083
62. Hutteman M, van der Vorst JR, Mieog JS et al (2011) Near-infrared fluorescence imaging in patients undergoing pancreaticoduodenectomy. Eur Surg Res 47:90–97
63. Desgrosellier JS, Cheresh DA (2010) Integrins in cancer: biological implications and therapeutic opportunities. Nat Rev Cancer 10:9–22
64. Hausner SH, Bauer N, Hu LY et al (2015) The effect of bi-terminal PEGylation of an integrin alphavbeta(6)-targeted (1)(8)F peptide on pharmacokinetics and tumor uptake. J Nucl Med 56:784–790
65. Hausner SH, Abbey CK, Bold RJ et al (2009) Targeted *in vivo* imaging of integrin alphavbeta6 with an improved radiotracer and its relevance in a pancreatic tumor model. Cancer Res 69:5843–5850
66. Liu Z, Liu H, Ma T et al (2014) Integrin alphavbeta(6)-targeted SPECT imaging for pancreatic cancer detection. J Nucl Med 55:989–994
67. Gao D, Gao L, Zhang C et al (2015) A near-infrared phthalocyanine dye-labeled agent for integrin alphavbeta6-targeted theranostics of pancreatic cancer. Biomaterials 53:229–238

68. Hackel BJ, Kimura RH, Miao Z et al (2013) 18F-fluorobenzoate-labeled cystine knot peptides for PET imaging of integrin alphavbeta6. J Nucl Med 54:1101–1105
69. Hammarstrom S (1999) The carcinoembryonic antigen (CEA) family: structures, suggested functions and expression in normal and malignant tissues. Semin Cancer Biol 9:67–81
70. Jessup M, Thomas P (1989) Carcinoembryonic antigen: function in metastasis by human colorectal carcinoma. Cancer Metastasis Rev 8:263–280
71. Boonstra MC, Verspaget HW, Ganesh S et al (2011) Clinical applications of the urokinase receptor (uPAR) for cancer patients. Curr Pharm Des 17:1890–1910
72. Maawy AA, Hiroshima Y, Zhang Y et al (2015) Near infra-red photoimmunotherapy with anti-CEA-IR700 results in extensive tumor lysis and a significant decrease in tumor burden in orthotopic mouse models of pancreatic cancer. PLoS One 10:e0121989
73. Hiroshima Y, Maawy A, Sato S et al (2014) Hand-held high-resolution fluorescence imaging system for fluorescence-guided surgery of patient and cell-line pancreatic tumors growing orthotopically in nude mice. J Surg Res 187:510–517
74. Metildi CA, Kaushal S, Luiken GA et al (2014) Advantages of fluorescence-guided laparoscopic surgery of pancreatic cancer labeled with fluorescent anti-carcinoembryonic antigen antibodies in an orthotopic mouse model. J Am Coll Surg 219:132–141
75. Metildi CA, Kaushal S, Pu M et al (2014) Fluorescence-guided surgery with a fluorophore-conjugated antibody to carcinoembryonic antigen (CEA), that highlights the tumor, improves surgical resection and increases survival in orthotopic mouse models of human pancreatic cancer. Ann Surg Oncol 21:1405–1411
76. Tran Cao HS, Kaushal S, Metildi CA et al (2012) Tumor-specific fluorescence antibody imaging enables accurate staging laparoscopy in an orthotopic model of pancreatic cancer. Hepatogastroenterology 59:1994–1999
77. Kaushal S, McElroy MK, Luiken GA et al (2008) Fluorophore-conjugated anti-CEA antibody for the intraoperative imaging of pancreatic and colorectal cancer. J Gastrointest Surg 12:1938–1950
78. Girgis MD, Olafsen T, Kenanova V et al (2011) Targeting CEA in pancreas cancer xenografts with a mutated scFv-Fc antibody fragment. EJNMMI Res 1:24
79. Peruzzi B, Bottaro DP (2006) Targeting the c-Met signaling pathway in cancer. Clin Cancer Res 12:3657–3660
80. Normanno N, De Luca A, Bianco C et al (2006) Epidermal growth factor receptor (EGFR) signaling in cancer. Gene 366:2–16
81. Voldborg BR, Damstrup L, Spang-Thomsen M, Poulsen HS (1997) Epidermal growth factor receptor (EGFR) and EGFR mutations, function and possible role in clinical trials. Ann Oncol 8:1197–1206
82. Boyle AJ, Cao PJ, Hedley DW et al (2015) MicroPET/CT imaging of patient-derived pancreatic cancer xenografts implanted subcutaneously or orthotopically in NOD-scid mice using (64)Cu-NOTA-panitumumab F(ab')2 fragments. Nucl Med Biol 42:71–77
83. Hudson SV, Huang JS, Yin W et al (2014) Targeted noninvasive imaging of EGFR-expressing orthotopic pancreatic cancer using multispectral optoacoustic tomography. Cancer Res 74:6271–6279
84. Wang L, Zhong X, Qian W et al (2014) Ultrashort Echo Time (UTE) imaging of receptor targeted magnetic iron oxide nanoparticles in mouse tumor models. J Magn Reson Imaging 40:1071–1081
85. Yang L, Mao H, Wang YA et al (2009) Single chain epidermal growth factor receptor antibody conjugated nanoparticles for *in vivo* tumor targeting and imaging. Small 5:235–243
86. Nayak TK, Regino CA, Wong KJ et al (2010) PET imaging of HER1-expressing xenografts in mice with 86Y-CHX-A"-DTPA-cetuximab. Eur J Nucl Med Mol Imaging 37:1368–1376
87. Munz M, Baeuerle PA, Gires O (2009) The emerging role of EpCAM in cancer and stem cell signaling. Cancer Res 69:5627–5629
88. Huang SM, Harari PM (1999) Epidermal growth factor receptor inhibition in cancer therapy: biology, rationale and preliminary clinical results. Invest New Drugs 17:259–269
89. Milenic DE, Wong KJ, Baidoo KE et al (2010) Targeting HER2: a report on the *in vitro* and *in vivo* pre-clinical data supporting trastuzumab as a radioimmunoconjugate for clinical trials. MAbs 2:550–564
90. Smith HW, Marshall CJ (2010) Regulation of cell signalling by uPAR. Nat Rev Mol Cell Biol 11:23–36
91. Yang L, Sajja HK, Cao Z et al (2013) uPAR-targeted optical imaging contrasts as theranostic agents for tumor margin detection. Theranostics 4:106–118
92. Lee GY, Qian WP, Wang L et al (2013) Theranostic nanoparticles with controlled release of gemcitabine for targeted therapy and MRI of pancreatic cancer. ACS Nano 7:2078–2089
93. Yang L, Mao H, Cao Z et al (2009) Molecular imaging of pancreatic cancer in an animal model using targeted multifunctional nanoparticles. Gastroenterology 136:1514–1525, **e1512**
94. Dullin C, Zientkowska M, Napp J et al (2009) Semiautomatic landmark-based two-dimensional-three-dimensional image fusion in living mice: correlation of near-infrared fluorescence imaging of Cy5.5-labeled antibodies with flat-panel volume computed tomography. Mol Imaging 8:2–14
95. Goel HL, Mercurio AM (2013) VEGF targets the tumour cell. Nat Rev Cancer 13:871–882
96. Pysz MA, Machtaler SB, Seeley ES et al (2015) Vascular endothelial growth factor receptor type 2-targeted contrast-enhanced US of pancreatic cancer neovasculature in a genetically engineered mouse model: potential for earlier detection. Radiology 274:790–799
97. Deshpande N, Ren Y, Foygel K et al (2011) Tumor angiogenic marker expression levels during tumor growth: longitudinal assessment with molecularly targeted microbubbles and US imaging. Radiology 258:804–811
98. Korpanty G, Carbon JG, Grayburn PA et al (2007) Monitoring response to anticancer therapy by targeting microbubbles to tumor vasculature. Clin Cancer Res 13:323–330
99. Humphries MJ (2000) Integrin cell adhesion receptors and the concept of agonism. Trends Pharmacol Sci 21:29–32
100. Martin-Bermudo MD (2000) Integrins modulate the Egfr signaling pathway to regulate tendon cell differentiation in the Drosophila embryo. Development 127:2607–2615
101. Gold P, Freedman SO (1965) Specific carcinoembryonic antigens of the human digestive system. J Exp Med 122:467–481
102. Ford CHJ, Tsaltas GC, Osborne PA, Addetia K (1996) Novel flow cytometric analysis of the progress and route of internalization of a monoclonal anti-carcinoembryonic antigen (CEA) antibody. Cytometry 23:228–240
103. Higazi AAR, Cohen RL, Henkin J et al (1995) Enhancement of the enzymatic activity of single-chain urokinase plasminogen activator by soluble urokinase receptor. J Biol Chem 270:17375–17380
104. Vilhardt F, Nielsen M, Sandvig K, van Deurs B (1999) Urokinase-type plasminogen activator receptor is internalized by different mechanisms in polarized and nonpolarized Madin-Darby canine kidney epithelial cells. Mol Biol Cell 10:179–195
105. Birchmeier C, Birchmeier W, Gherardi E, Vande Woude GF (2003) Met, metastasis, motility and more. Nat Rev Mol Cell Biol 4:915–925
106. Wiehr S, von Ahsen O, Rose L et al (2013) Preclinical evaluation of a novel c-Met inhibitor in a gastric cancer xenograft model using small animal PET. Mol Imaging Biol 15:203–211
107. Timofeevski SL, McTigue MA, Ryan K et al (2009) Enzymatic characterization of c-Met receptor tyrosine kinase oncogenic mutants and kinetic studies with aminopyridine and triazolopyrazine inhibitors. Biochemistry 48:5339–5349
108. Naka D, Shimomura T, Yoshiyama Y et al (1993) Internalization and degradation of hepatocyte growth factor in hepatocytes with down-regulation of the receptor/c-Met. FEBS Lett 329:147–152
109. Kari C, Chan TO, Rocha de Quadros M, Rodeck U (2003) Targeting the epidermal growth factor receptor in cancer: apoptosis takes center stage. Cancer Res 63:1–5
110. Dadparvar S, Krishna L, Miyamoto C et al (1994) Indium-111-labeled anti-EGFr-425 scintigraphy in the detection of malignant gliomas. Cancer 73:884–889
111. Harding J, Burtness B (2005) Cetuximab: an epidermal growth factor receptor chemeric human-murine monoclonal antibody. Drugs Today (Barc) 41:107–127
112. Akiyama T, Sudo C, Ogawara H, Toyoshima K, Yamamoto T (1986) The product of the human c-erbB-2 gene: a 185-kilodalton glycoprotein with tyrosine kinase activity. Science 232:1644–1646
113. Guillemard V, Nedev HN, Berezov A, Murali R, Saragovi HU (2005) HER2-mediated internalization of a targeted prodrug cytotoxic conjugate is dependent on the valency of the targeting ligand. DNA Cell Biol 24:350–358
114. Jain RK (2002) Tumor angiogenesis and accessibility: role of vascular endothelial growth factor. Semin Oncol 29:3–9

115. Paudyal B, Paudyal P, Shah D et al (2014) Detection of vascular endothelial growth factor in colon cancer xenografts using bevacizumab based near infrared fluorophore conjugate. J Biomed Sci 21:35
116. Jankowski V, Schulz A, Kretschmer A et al (2013) The enzymatic activity of the VEGFR2 receptor for the biosynthesis of dinucleoside polyphosphates. J Mol Med (Berl) 91:1095–1107
117. Santos SC, Miguel C, Domingues I et al (2007) VEGF and VEGFR-2 (KDR) internalization is required for endothelial recovery during wound healing. Exp Cell Res 313:1561–1574
118. Armstrong A, Eck SL (2003) EpCAM: A new therapeutic target for an old cancer antigen. Cancer Biol Ther 2:320–326
119. Zhu B, Wu G, Robinson H et al (2013) Tumor margin detection using quantitative NIRF molecular imaging targeting EpCAM validated by far red gene reporter iRFP. Mol Imaging Biol 15:560–568
120. Lund K, Bostad M, Skarpen E et al (2014) The novel EpCAM-targeting monoclonal antibody 3–17I linked to saporin is highly cytotoxic after photochemical internalization in breast, pancreas and colon cancer cell lines. MAbs 6:1038–1050